ARTICLE
Journal of Cellular Biochemistry 113:2167–2177 (2012)

Journal of Cellular Biochemistry

HDAC2 Overexpression Confers Oncogenic Potential to Human Lung Cancer Cells by Deregulating Expression of Apoptosis and Cell Cycle Proteins

Kwang Hwa Jung,[1,2] Ji Heon Noh,[1,2] Jeong Kyu Kim,[1,2] Jung Woo Eun,[1,2] Hyun Jin Bae,[1,2] Hong Jian Xie,[1,2] Young Gyoon Chang,[1,2] Min Gyu Kim,[1,2] Hanna Park,[1,2] Jung Young Lee,[1,2] and Suk Woo Nam[1,2]*

[1]*Department of Pathology, College of Medicine and Functional RNomics Research Center, The Catholic University of Korea, Banpo-dong, Seocho-gu, Seoul, Korea*

[2]*Functional RNomics Research Center, The Catholic University of Korea, Seoul, Korea*

ABSTRACT

Histone deacetylase 2 (HDAC2) is crucial for embryonic development, affects cytokine signaling relevant for immune responses, and is often significantly overexpressed in solid tumors, but little is known of its role in human lung cancer. In this study, we demonstrated the aberrant expression of HDAC2 in lung cancer tissues and investigated oncogenic properties of HDAC2 in human lung cancer cell lines. HDAC2 inactivation resulted in regression of tumor cell growth and activation of cellular apoptosis via p53 and Bax activation and Bcl2 suppression. In cell cycle regulation, HDAC2 inactivation caused induction of $p21^{WAF1/CIP1}$ expression, and simultaneously suppressed the expressions of cyclin E2, cyclin D1, and CDK2, respectively. Consequently, this led to the hypophosphorylation of pRb protein in G1/S transition and thereby inactivated E2F/DP1 target gene transcriptions of A549 cells. In addition, we demonstrated that HDAC2 directly regulated $p21^{WAF1/CIP1}$ expression in a p53-independent manner. However, HDAC1 was not related to $p21^{WAF1/CIP1}$ expression and tumorigenesis of lung cancer. Lastly, we observed that sustained-suppression of HDAC2 in A549 lung cancer cells attenuated in vitro tumorigenic properties and in vivo tumor growth of the mouse xenograft model. Taken together, we suggest that the aberrant regulation of HDAC2 and its epigenetic regulation of gene transcription in apoptosis and cell cycle components play an important role in the development of lung cancer. J. Cell. Biochem. 113: 2167–2177, 2012.

KEY WORDS: HDAC2; APOPTOSIS; CELL CYCLE; $P21^{WAF1/CIP1}$; LUNG CANCER

Histone acetylation is a major modification that affects gene transcription and is controlled by histone acetyltransferases (HATs). Histone deacetylases (HDACs), which remove the acetyl groups from hyperacetylated histones, counteract the effects of HATs, and return histone to its basal state, with the concomitant suppression of gene transcription [Marks et al., 2001a]. There is clear evidence for the involvement of both HATs and HDACs in cell proliferation, differentiation, and cell cycle regulation [Minucci and Pelicci, 2006]. Hence, the dysregulation of acetylation status in the cell is closely linked to cancer [Kortenhorst et al., 2006; Yang and Seto, 2007]. Although there is clear evidence for the involvement of HDACs in the development of cancer, the specific roles of individual HDACs in the regulation of cell proliferation, apoptosis, and cell cycle are unclear. The HDAC inhibitors used to demonstrate effects on cells are for the most part non-specific for the different HDAC isoforms [Marks et al., 2001b; Johnstone, 2002]. There are 18 HDACs, which are generally divided into four classes, based on sequence homology to yeast counterparts [Glozak and Seto, 2007]. Class I includes HDAC1, 2, 3, and 8, which bear significant homology to the yeast protein RPD3 and are mainly localized to the nucleus. Class II includes HDAC4–7, 9, and 10, which are homologous to yeast HAD-1-like enzymes and shuttle between

Additional supporting information may be found in the online version of this article.

Grant sponsor: Basic Science Research and Public Welfare & Safety programs through National Research Foundation of Korea (NRF) funded by the Ministry of Education, Science and Technology; Grant numbers: 2009-0072504, 2010-0020764.

*Correspondence to: Prof. Suk Woo Nam, Department of Pathology, College of Medicine and Functional RNomics Research Center, The Catholic University of Korea, 505 Banpo-dong, Seocho-gu, Seoul 137-701, Korea.
E-mail: swnam@catholic.ac.kr

Manuscript Received: 6 October 2011; Manuscript Accepted: 27 January 2012
Accepted manuscript online in Wiley Online Library (wileyonlinelibrary.com): 3 February 2012
DOI 10.1002/jcb.24090 • © 2012 Wiley Periodicals, Inc.

nucleus and cytoplasm. Class III, the NAD^+-dependent HDACs, comprises SIRT1-7, which show similarity to yeast SIR2. Class IV comprises HDAC11, which has some features of both classes I and II HDACs [Gregoretti et al., 2004]. Despite the increasing number of HDAC enzymes isolated from different species, the specialized functions of most HDACs are unknown. Also, the regulation of these enzymes during cell cycle and proliferation is largely unknown.

HDAC2 is found in large protein complexes, which are associated with nuclear receptor corepressor and ligand-dependent corepressor, such as NuRD and mSin3 [Zhang et al., 1999; Fernandes et al., 2003]. A previous study has suggested that increased HDAC2 expression was found and is enhanced by loss of APC in human colorectal cancer [Zhu et al., 2004]. Also, there have been reports suggesting that overexpression of HDAC2 was found in stomach cancer and hepatocellular carcinomas suggesting an important role of HDAC2 in the development and progression of these cancers [Song et al., 2005b; Noh et al., 2006]. In addition, it has been reported that inhibition of HDAC2 increased the apoptotic response and $p21^{WAF1/CIP1}$ expression in HeLa cells [Huang et al., 2005]. In lung cancer, it has been suggested that expression of HDAC2 was associated with large cell type of non-small cell lung carcinoma [Borczuk et al., 2003]. However, no attempt has been made so far to explain the underlying mechanisms responsible for the oncogenic potential of HDAC2 in apoptosis and cell cycle regulation of lung cancer.

In this study, to investigate the oncogenic potential of HDAC2 in lung cancer, we assessed the aberrant expression of HDAC2 in lung cancer, and examined the regulatory mechanisms of HDAC2 in apoptosis and cell cycle, especially in G1/S transition of human lung cancer cell lines. In addition, the tumorigenic potential of HDAC2 in vitro and in vivo was experimentally explored using stable HDAC2 knockdown cell lines.

MATERIALS AND METHODS

ETHICS STATEMENT

A total of 35 (12 adenocarcinomas, 6 basaloid carcinomas, 6 squamous cell carcinomas, 6 large cell carcinomas, and 5 solid type adenocarcinomas) formalin-fixed, paraffin-embedded non-small cell lung cancer samples were obtained from surgical resection at the College of Medicine of Catholic University of Korea through an IRB approved protocol (CUMC11U009). Written informed consent was obtained from all patients. All animal experiments were performed in compliance with the guidelines of the Department of Laboratory Animal, IACUC in College of Medicine, The Catholic University of Korea (CUMC-2009-0050-03).

TISSUE MICROARRAY AND IMMUNOHISTOCHEMICAL ANALYSIS OF HDAC2

Lung cancer tissue microarray (TMA) was constructed using the device previously described by Kononen et al. [1998]. To investigate the aberrant regulation of HDAC2 in lung cancer, we performed immunohistochemical staining with polyclonal antibody against HDAC2 (1:100; Santa Cruz Biotechnology, Delaware, CA) in lung cancer TMA. Prior to immunostaining, the TMA slides were deparaffinized and hydrated through graded ethanol to deionized water. As negative control, the slides were treated with replacement of the primary antibody by non-immune serum. Scoring of the TMA was performed independently by two pathologists. In the event of disagreement, the two pathologists reached a consensus by jointly reevaluating the TMA using a multi-head microscope. Immunostaining intensity was graded in three categories: 1+ (weak), 2+ (moderate), or 3+ (strong). However, if the number of immunostained cells was less than 10%, we considered this case as negative. The duplicate core tumor tissues were combined and calculated as one case.

CELL CULTURE

Human lung carcinoma cell line A549, NCI-H358, and NCI-H460 were purchased from American Type Culture Collection (ATCC). Cells were cultured in RPMI-1640 and DMEM supplemented with 10% fetal bovine serum (Sigma, St Louis, MO) and 1 mg/ml of penicillin/streptomycin (Invitrogen, Carlsbad, CA).

QUANTITATIVE REAL TIME REVERSE TRANSCRIPTASE-PCR

Total RNA was extracted using TRIzol (Invitrogen) from A549 lung cancer cell line and quality control was performed using RNA 6000 Nano chips on an Agilent 2001 Bioanalyzer (Agilent Technologies, Palo Alto, CA). Then, 1 μg RNA was used for cDNA synthesis reaction using RNA PCR Core Kit (Roche Applied Science, Indianapolis, IN). Primer sequences are described in Supplementary Table I. Real-time PCR was conducted using the iQ™ 5 Real-Time PCR Detection System (Bio-Rad Laboratories, Hercules, CA) in accordance to the manufacturer's instructions. An average Ct (threshold cycle) value from triplicate assays was used for further calculation, and the normalized expression level using glyceraldehyde-3-phosphate dehydrogenase (GAPDH) as the reference.

ENDOGENOUS KNOCKDOWN OF HDAC2 AND ESTABLISHMENT OF HDAC2 KNOCKDOWN CELL LINES

HDAC2 siRNA and the negative control siRNA (scrambled siRNA) were purchased from Ambion Inc (Bedford, MA). The targeted *HDAC2* sequences were 5′-GGAAGAAGAUAAAUCCAAGTT-3′ (Sense) and 5′-CUUGGAUUUAUCUUCUUCCTT-3′ (Antisense). A549 cells were transfected with 100 nM or 200 nM of HDAC2-specific siRNA in 250 μl of Opti-MEM (Invitrogen). Transfection was carried out using 6 μl of lipofectamine 2000 reagent (Invitrogen) according to the manufacturer's specifications. The pSilencer™ 3.1-H1 neo plasmid (Ambion) was used for the construction of shRNA-encoding plasmids. To establish the HDAC2 knockdown cell lines, the pSilencer-HDAC2 shRNA vector was transfected into cells by Lipofectamine 2000 reagent (Invitrogen) according to the manufacturer's protocol. After selection in G418 (0.5 mg/ml) for 2 weeks, cells were plated into 10 cm dishes at limiting cell dilutions. Single cells that grew into individual colonies were removed from the dish by cell scraping and transferred into a twenty four-well plate. Each cell line was then expanded and was strictly maintained in the same concentrations of G418 to avoid reversion of the cells. Validation of silencing of HDAC2 protein expression was performed by Western blot analysis.

CELL PROLIFERATION ASSAY

For cell proliferation assay, cells were plated in 6-well plates at a density of 4×10^4 cells per well with RPMI-1640 medium with 10% FBS and maintained for 16∼18Yh. Four hours after siRNA transfection, cells were incubated with 5 mg/ml of the yellow MTT-[3-(4,5-dimethylthiazol-2-yl)-2,5-diphenyltetrazolium bromide] solution at the each indicated time point. One hour after incubation, dark blue formazan products were dissolved in dimethyl sulfoxide (DMSO, Sigma) and absorbance of the cells were determined with a VICTOR3^{TM} Multilabel Plate Reader (PerkinElmer Inc, Boston, MA).

THYMIDINE INCORPORATION ASSAY

Incorporation of [^{3}H] thymidine into DNA was used to determine the effect of HDAC2 knockdown on the A549 lung cancer cell line in vitro. To measure [^{3}H] thymidine incorporation assay, all the subsequent steps were performed as described below. The cells were labeled for the last 9Yh with 1 μCi/ml [^{3}H] thymidine (Nen life sciences, Boston, MA) per well and incubated at 37°C for the each indicated time point. After incubation, the cells were fixed with ice-cold 5% trichloroacetic acid. This was removed, and cells were solubilized by adding 0.2 M sodium hydroxide and 1% (w/v) SDS. Plates were incubated at room temperature for 5 min, after which the solubilized contents of cells were transferred into scintillation vials and radioactivity was determined by liquid scintillation counting.

WESTERN BLOT ANALYSIS

Whole-cell extracts were prepared with radio immunoprecipitation assay (RIPA) buffer (50 mmol/L Tris-HCl [pH7.4], 150 mmol/L NaCl, 1% Nonidet P-40, 0.25% sodium deoxycholate, 1 mmol/L Phenylmethane-sulfonylfluoride containing protease inhibitors, Roche Molecular Biochemicals, Mannheim, Germany). The characteristics of primary antibodies used are listed in Supplementary Table II. The membrane was exposed to LAS 3000 (Fuji, Japan).

APOPTOSIS ASSAY

The Annexin V-FITC Apoptosis Detection Kit I (BD Biosciences, San Jose, CA) was used to quantify the level of apoptosis in the samples. Briefly, the cells were trypsinized, washed twice with cold PBS, and resuspended in 1X binding buffer at a concentration of 1×10^6 cells/ml. The cells were transferred, 100 μl of the cell suspension (1×10^5 cells) to a 5 ml culture tube and 5 μl of annexin V-FITC and 10 μl of PI solution was added. After 15 min of incubation at room temperature in the dark, 400 μl of 1X binding buffer was added to each of the culture tubes; determination of the apoptotic fraction of cells was then performed by Cell-Quest FACS analysis software on the flow cytometer FACScan (BD Biosciences).

SOFT AGAR COLONY FORMATION ASSAY

For soft agar assay, HDAC2 knocked down A549 clones (3,000 cells per dish) in 1 ml of 0.4% agarose with RPMI-1640 were plated in each well on the top of existing 0.8% bottom agarose in 35-mm dishes in triplicate for each treatment condition. The covering medium was replaced every week. At the end of 4 weeks, cell colonies were stained with 0.05% crystal violet and colonies >0.1 mm in diameter were counted under a microscopic field at ×40 magnifications.

CELL MOTILITY ASSAY

Motility assays of HDAC2 knocked down A549 clones and were performed in 48-well modified Boyden chambers (Neuroprobe, Cabin John, MD) as described previously [Song et al., 2005a].

TUMOR XENOGRAFT ASSAY

For the xenograft tumorigenesis assay, 5×10^6 cells of the indicated cell lines were mixed with 0.2 ml phosphate buffer saline (PBS, pH 7.4) and the cell suspension was injected s.c into the flank of 4-week-old male athymic nude mice. Mice that were injected with non-transfected A549 cells were the control group; mice that were injected with A549 cells transfected with empty-vector were the Mock group; mice that were injected with HDAC2 knocked down A549 clones, HD2 KD1 or HD2 KD2 cells were sustained HDAC2 suppression group. Mice were examined two or three times per week for tumor formation at the sites of injection. Tumor volume was calculated according to the formula: $0.5 \times \text{length} \times \text{width}^2$. Each experimental group consisted of five mice and tumor growth was quantified by measuring the tumors with calipers in three dimensions. The results were expressed as the mean tumor volume with 95% confidence intervals.

STATISTICAL ANALYSIS

The immunohistochemical staining of lung tumor sub-type TMA was assessed using the chi-square test. For the cell proliferation, thymidine incorporation, soft agar colony formation, and cell motility assay, the statistical evaluation of the data was determined by mean ± standard deviation (SD) of three experiments by use of Prism 4.00 (GraphPad Software). $P < 0.05$ was considered statistically significant.

RESULTS

ABERRANT EXPRESSION OF HDAC2 IN HUMAN LUNG CANCER

To investigate the dysregulation of HDAC2 in lung cancer, immunohistochemical staining of human lung cancer TMA with HDAC2 antibody was performed. Immunostaining results of the replicated tumor specimens in the TMA are summarized in Table I. and the representative images of immunostaining are shown in Figure 1. HDAC2 was localized predominantly in the nucleus in all cases of non-small cell lung cancer except for in one negative case of solid type adenocarcinoma (Fig. 1B). In the lung cancer tissues, 22 cases showed strong immunopositivity (62.9%), 5 cases showed moderate immunopositivity (14.3%), and 7 cases showed weak immunopositivity (20%). As shown in Table I, there were no significant differences in HDAC2 expression among the histologic subtypes of non-small cell lung cancer (NSCLC). HDAC2 was also detectable in the normal bronchial ciliated epithelial cells, peribronchial glands, and alveolar pneumocytes but was very weak and was mainly localized in the nucleus. Interstitial and lymphoid cells in areas adjacent to tumors were also occasionally immunostained but were weakly stained in cytoplasm and nucleus. In normal tissues, 27 cases showed 1+ immunoreactivity (77.1%)

TABLE I. Results for HDAC2 Immunohistochemistry According to Tumor Sub-Type Tissue Microarray

HDAC2	0	1	2	3
Adenocarcinoma (12)				
Normal	2 (16.7%)	10 (83.3%)	0 (0%)	0 (0%)
Tumor	0 (0%)	5 (41.7%)	1 (8.3%)	6 (50%)
HDAC2	0	1	2	3
Solid type adenocarcinoma (5)				
Normal	1 (20%)	4 (80%)	0 (0%)	0 (0%)
Tumor	1 (20%)	0 (0%)	1 (20%)	3 (60%)
HDAC2	0	1	2	3
Large cell carcinoma (6)				
Normal	2 (33.3%)	4 (66.7%)	0 (0%)	0 (0%)
Tumor	0 (20%)	1 (16.7%)	1 (16.7%)	4 (66.6%)
HDAC2	0	1	2	3
Squamous cell carcinoma (6)				
Normal	1 (16.7%)	5 (83.3%)	0 (0%)	0 (0%)
Tumor	0 (0%)	0 (0%)	1 (16.7%)	5 (83.3%)
HDAC2	0	1	2	3
Basaloid carcinoma (6)				
Normal	2 (33.3%)	4 (66.7%)	0 (0%)	0 (0%)
Tumor	0 (0%)	1 (16.7%)	1 (16.7%)	4 (66.7%)
Total	≤ 1	≥ 2		
Normal*	35 (100%)	0 (0%)	†$P < 0.0001$	
Tumor*	8 (22.9%)	27 (77.1%)		

*Number of samples showing an increase of ≤ 1 and ≥ 2 in scores for each of normal and tumor samples. Data are given as number of patients (%) when otherwise indicated.
†Chi-squre test.

and 8 cases were immunonegative (22.9%). And none of the normal lung tissues were scored 2+ or 3+ for HDAC2 expression. In contrast, 27 out of the 35 cases (77.1%) of lung cancer tissues were scored 2+ or 3+ for HDAC2 expression. This result indicated that HDAC2 was dysregulated and overexpressed in lung cancer.

SUPPRESSION OF HDAC2 ELICITS ANTI-MITOGENIC POTENTIAL IN A549 HUMAN LUNG CANCER CELLS

Immunohistochemical analysis of HDAC2 showed aberrant expression of HDAC2 in NSCLC. To verify aberrant regulation of HDAC2 among HDACs, we assessed the endogenous expression level of HDACs in A549 cells by quantitative real-time PCR using specific primers for some of the available HDACs (HDAC1∼8). As shown in Figure 2A, the endogenous expression of HDAC2 mRNA was relatively high among the HDACs. To confirm this aberrant regulation of HDAC2 in lung cancer cell line, we performed same experiment with another lung cancer cell line, NCI-H358, and found that endogenous expression of HDAC2 was highest among the tested HDACs (Supplementary Fig. S1). This indicated that HDAC2 is selectively deregulated in lung cancer. Next, to explain the biological consequences of the aberrant expression of HDAC2 in lung cancer, HDAC2 was abrogated by the RNA interference-mediated protein knockdown method. As shown in Figure 2B, the growth rate of HDAC2 siRNA-transfected cells appeared to be

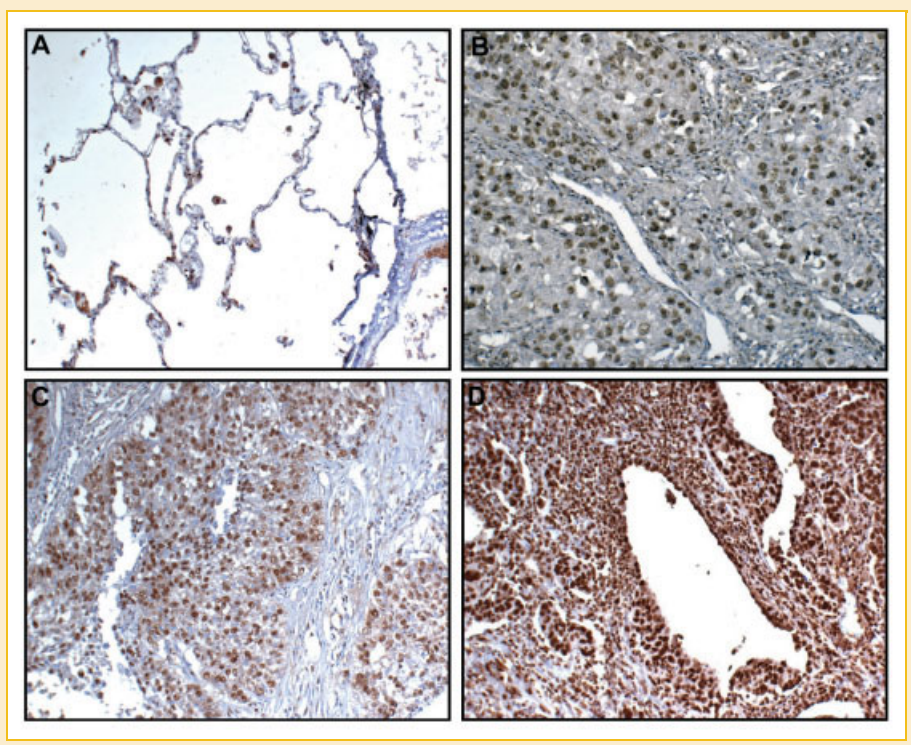

Fig. 1. Immunohistochemical analysis of HDAC2 expression in human non-small cell lung cancer. A: Normal lung tissue shows negative staining for HDAC2 expression with 1+ positive immunostaining in normal alveolar macrophages. B: An example of adenocarcinoma, solid type, showing negative staining for HDAC2 expression. C: An example of squamous cell carcinoma, showing 2+ staining intensity with 1+ stromal cells. D: An example of adenocarcinoma showing 3+ staining for HDAC2. Original magnifications, ×200. Two experiments with the same results were performed.

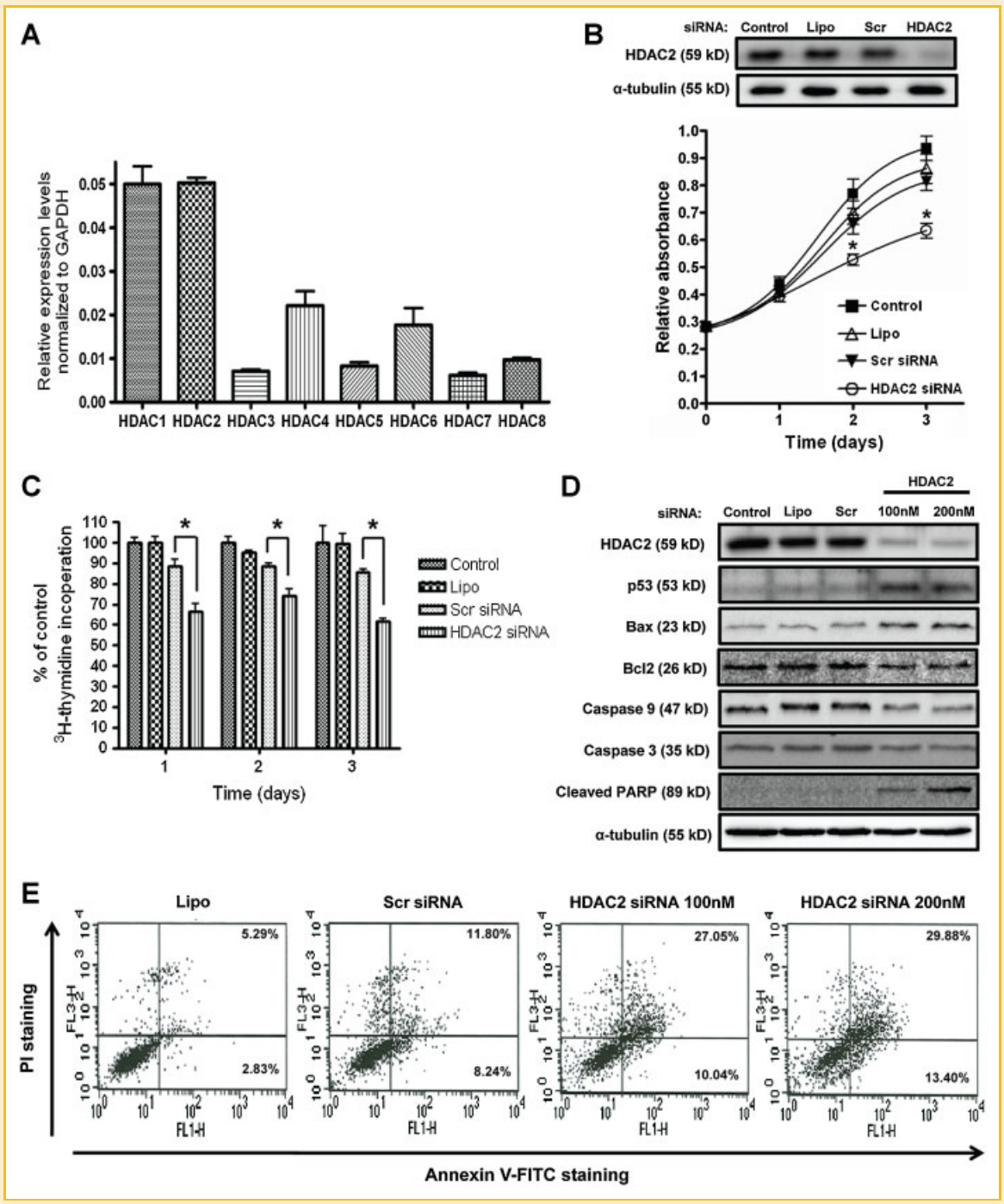

Fig. 2. Effect of HDAC2 knockdown on cell proliferation and apoptosis in A549 cells. A: Endogenous expression of HDACs in A549 cells measured by quantitative real-time reverse transcriptase PCR. HDAC mRNA levels were normalized against GAPDH and graph bars show the relative expression of HDACs in A549 cells. Each experiment was performed in triplicate. Error bars show mean ± SD. B: The tumor cell growth rates were assessed by MTT cell viability assay in A549 cells transfected with none (Control), lipofectamine only (Lipo), 100 nmol/L scrambled siRNA (Scr siRNA), 100 nmol/L HDAC2-specific siRNA (HDAC2 siRNA). The relative growth rate was determined by MTT assay at the each indicated time point. For western blot analysis, expression of α-tubulin was used as a protein loading control. Error bars indicate mean ± SD of three experiments. Significant differences between the Scr and HDAC2 siRNA transfected groups are indicated: $^{*}P < 0.05$, unpaired Student's *t* test. C: The effect of HDAC2 depletion on de novo DNA synthesis was measured by [3H]-thymidine incorporation assay. Results are expressed as a percentage of control. Error bars show mean ± SD of three experiments. (unpaired Student's *t* test, $^{*}P < 0.05$ vs. Scr siRNA). D: Abrogation of HDAC2 induces activation of cellular apoptosis. Some major components of mitochondrial control of apoptosis were analyzed in the cells transfected with none (control), lipofectamine only (Lipo), 100 nmol/L scrambled siRNA (Scr siRNA), 100 nmol/L, and 200 nmol/L HDAC2 siRNA. All experiments were repeated three times with same results. A typical result of three performed experiments is shown. E: Flow cytometric analysis of A549 cells transfected with lipofectamine only (Lipo), 100 nmol/L scrambled siRNA (Scr siRNA), 100 nmol/L, and 200 nmol/L HDAC2 siRNA. The flow cytometric analysis was measured through Annexin V labeling and PI staining on suppression of HDAC2. Double staining with Annexin V and PI indicates the cells in the late stage of apoptosis (Upper right). Two independent with the same results were performed.

regressed as compared to non-transfectant (Control or Lipo) or scrambled sequence of siRNA transfectants (Scr). At 3 days after transfection, the growth rate of HDAC2 siRNA-transfected cells was regressed by 35% than that of the non-transfection group, while the growth rate of the cells transfected with scrambled siRNA sequence or transfection reagent only (Lipo) appeared to be slightly decreased as compared to the non-transfectant cells (Fig. 2B). In addition, we also observed that de novo DNA synthesis was significantly inhibited by HDAC2 knockdown in thymidine incorporation assay (Fig. 2C). These anti-mitogenic effects of HDAC2 inactivation could be partially explained by the disruption of cell growth regulation such as the cell cycle arrest, cellular senescence, or apoptosis. Thus, we next explored the effects of HDAC2 knockdown in cellular apoptosis and cell cycle regulation.

Mitochondrial control of cellular apoptosis balances between the activities of pro-apoptotic and anti-apoptotic components. As shown in Figure 2D, HDAC2 knockdown caused inductions of p53 and Bax expression and simultaneously suppressed Bcl2 expression. This suggests that the activation of p53 induces the transcriptional activation of Bax protein, a pro-apoptotic factor which is normally suppressed by Bcl2, an anti-apoptotic regulator. Consequently, basal levels of caspase-9 and -3 were decreased with the induction of cleavage form of PARP. This observation was also confirmed by the flow cytometric analysis of Annexin V staining cells in siRNA transfectants. As shown in Figure 2E, we observed a significant induction of apoptotic cells in the HDAC2 siRNA transfectants as compared to control groups (Lipo or Scr siRNA). The apoptotic cells (upper right of the dot plot graphs in Fig. 2E) increased to 27.05% and 29.88% in 100 nM and 200 nM of HDAC2 siRNA treatment, respectively, as compared to that in Lipo (5.29%) or Scr siRNA (11.80%) treatment. These results indicated that overexpression of HDAC2 disturbed the cellular balance of apoptosis thereby conferring resistance to apoptotic signal in lung cancer.

REGULATORY MECHANISMS OF HDAC2 ON G1/S TRANSITION OF THE CELL CYCLE IN LUNG CANCER CELLS

The fact that the suppression of HDAC2 caused regression of A549 lung cancer growth implies that HDAC2 is involved in the regulation of the cell cycle circuit. The cyclin dependent kinases (CDKs), CDK inhibitors (CDKIs), and cyclins are the core components of the cell cycle clock. Therefore, we next examined the effects of HDAC2 suppression on these regulatory components in the G1/S phase of cell cycle. As shown in Figure 3A, no significant changes were observed in the expression of $p15^{INK4B}$ and $p27^{Kip1}$ by HDAC2 knockdown. However, HDAC2 inactivation selectively induced $p21^{WAF1/CIP1}$ among negative regulators of cell cycle transition. In addition, HDAC2 knockdown also caused down-regulation of cyclin D1, cyclin E2, and CDK2 expressions (Fig. 3B). In general, the activated CDK/cyclin complex can cause hyperphosphorylation of pRb which loses its tumor suppressor activity, and allows for E2F/DP1 transcriptional activity. Thus, we next investigated whether this resulting dysregulation of CDK and cyclins by HDAC2 affects the E2F/DP1 transcriptional activity in A549 cells. As shown in Figure 3C, HDAC2 knockdown elicited hypophosphorylation of pRb without change in protein level of pRb thereby implying that the aberrant regulation of HDAC2 affects phosphorylation of pRb protein via transcriptional activation of CDK2, cyclin D1, and cyclin E2 in A549 cells. Further, we observed that some of the downstream target genes of E2F/DP1 transcription factor, such as E2F5, CDC2, and cyclin A, were down-regulated by HDAC2 suppression in A549 cells. This suggests that comprehensive regulation of $p21^{WAF1/CIP1}$, cyclin D1, cyclin E2, and CDK2 by HDAC2 overexpression exerts a

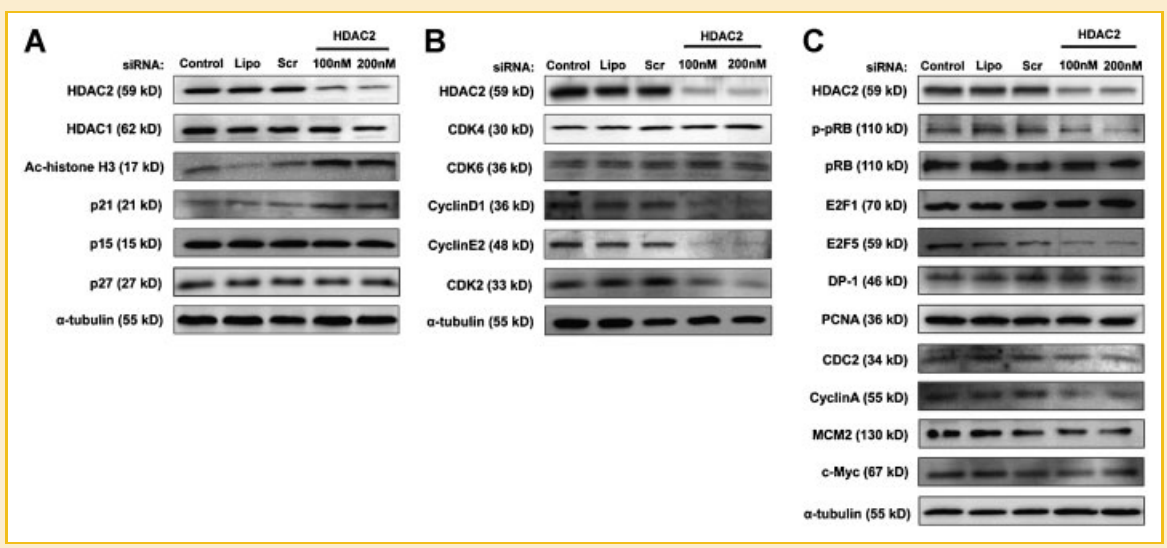

Fig. 3. HDAC2 regulates the expressions of regulatory components in G1/S cell-cycle transition. A549 cells were transfected with none (Control), lipofectamine only (Lipo), 100 nmol/L scrambled siRNA (Scr siRNA), 100 nmol/L, or 200nmol/L HDAC2-specific siRNA. A: Western blot analysis of negative regulators of G1/S cell-cycle transition by HDAC2 depletion in A549 cells. B: Effects of CDKs and cyclins in G1/S transition by HDAC2 depletion. C: Effects of HDAC2 depletion on pRb and E2F/DP1 target gene expressions. The α-tubulin was used as the protein loading control. All experiments were repeated three times with same results. A typical result of three performed experiments is shown.

very potent mitogenic stimulation causing uncontrolled cell growth during lung cancer progression.

Next, to generalize our findings, we employed two additional lung cancer cell lines and investigated whether these cell lines recapitulate the anti-mitotic effect of A549 cells upon HDAC2 inactivation. Among lung cancer cell lines, we selected NCI-H358 and NCI-H460 cell lines as they exhibited relatively high expression for HDAC2 in western blot analyses (data not shown). Then, each cell line was transfected with siRNA directed against HDAC2. As shown in Figure 4, the growth rate of HDAC2 knockdown cells appeared to be significantly regressed as compared to control or scr siRNA (transfectant with scramble sequence of siRNA) in both NCI-H358 and NCI-H460 cells. Concordant with previous observation in A549 cells, all cell lines displayed significant growth retardation upon HDAC2 knockdown. Additionally, both cell lines exhibited selective induction of $p21^{WAF1/CIP1}$ and suppression of cyclin D1 and CDK2 by HDAC2 inactivation providing consistent results that showed systemic modulation of cell cycle proteins by HDAC2 in A549 cells. These results strengthen our suggestion that aberrant overexpression of HDAC2 contributes mitotic potential to lung cancer cells during lung tumorigenesis.

HDAC2 DEPLETION INDUCES $P21^{WAF1/CIP1}$ EXPRESSION IN A P53-INDEPENDENT MANNER AND INDEPENDENT OF HDAC1 ACTIVITY

HDAC2 and HDAC1 share a high degree of homology and coexist within the same protein complexes. We also showed a relatively high expression of HDAC1 similar to HDAC2 in A549 cells (Fig. 2A). A previous study has reported that inhibition of HDAC2 increased apoptosis, and was associated with increased $p21^{WAF1/CIP1}$ expression that was independent of p53 and HDAC1 in HeLa cells [Huang et al., 2005]. Thus, to investigate whether HDAC2 regulates $p21^{WAF1/CIP1}$ by independent of p53 and HDAC1 in A549 lung cancer cells, we performed following experiments. As shown in Figure 5A, HDAC2 knockdown caused induction of both p53 and $p21^{WAF1/CIP1}$ expressions. Whereas ectopic expression of wild-type p53 (WT) or mutant-type p53 (R248W) did not affect $p21^{WAF1/CIP1}$ expression (Fig. 5A). Therefore, overexpression of HDAC2 seems independently to suppress both p53 and $p21^{WAF1/CIP1}$ expression in

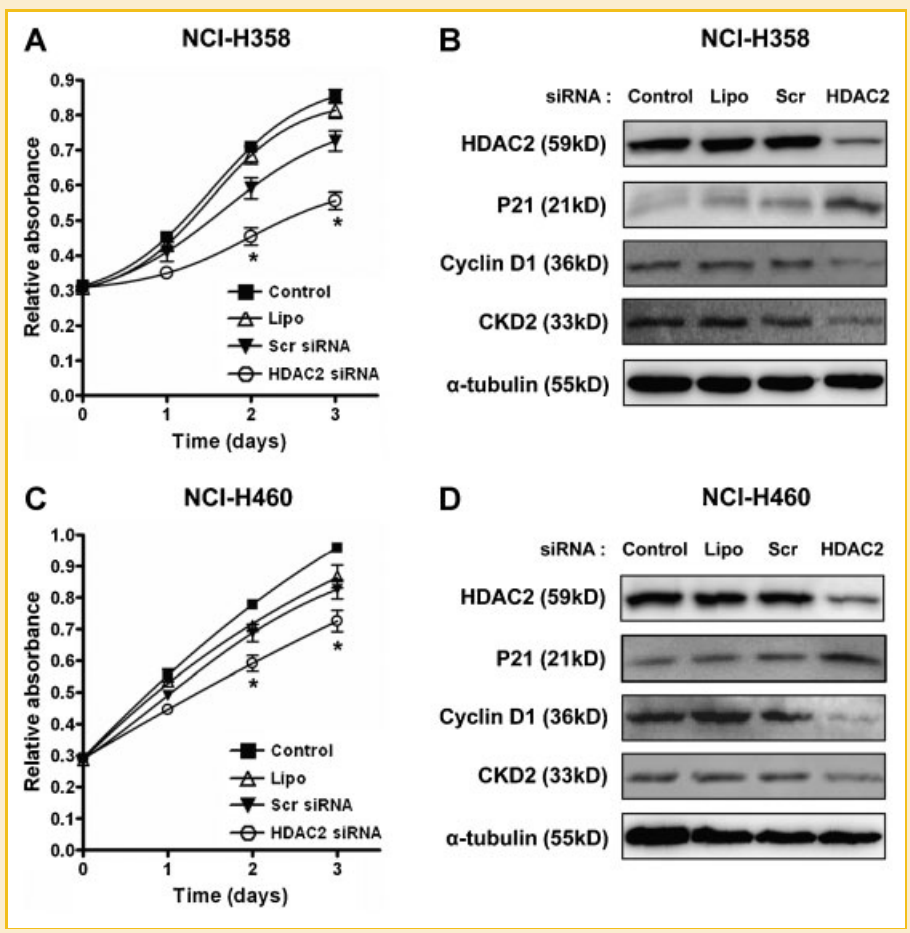

Fig. 4. Effect of HDAC2 knockdown on cell proliferation and G1/S cell-cycle transition in lung cancer cell lines. Upper panel, A: NCI-H358 and C: NCI-H460 cells were transfected with control (None), lipofectamine only (Lipo), 100 nmol/L scrambled siRNA (Scr siRNA), 100 nmol/L HDAC2-specific siRNA. The proliferation rates of lung cancer cell lines were determined by measuring MTT absorbance at A_{570} at the indicated times after transfection. Error bars show mean ± SD of three experiments (unpaired Student's *t* test, $^{*}P < 0.05$ vs. Scr siRNA). Lower panel, levels of $p21^{WAF1/CIP1}$, cyclin D1, and CDK2 by HDAC2 suppression in (B) NCI-H358 and (D) NCI-H460 cells were determined by western blot analysis. The α-tubulin was used as a loading control. Experiments were performed in duplicate.

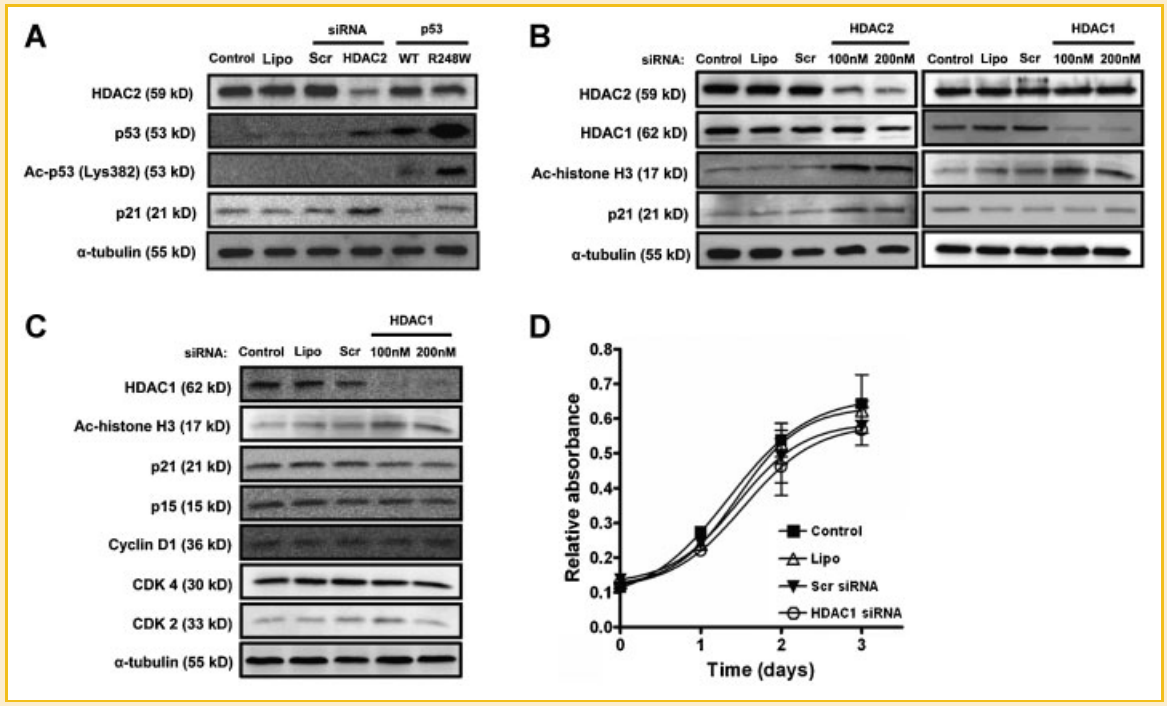

Fig. 5. Inhibition of HDAC2 induces $p21^{WAF1/CIP1}$ expression, in a p53-independent manner and independent of HDAC1 activity. Western blot analysis of A549 cells transfected with none (Control), lipofectamine only (Lipo), 100 nmol/L scrambled siRNA (Scr siRNA), 100 nmol/L, and 200 nmol/L of HDAC1 or HDAC2 siRNA and 1ug of wild-type p53 (WT) or 1ug of mutant p53 (R248W) plasmid. A: HDAC2 knockdown induced p53 and $p21^{WAF1/CIP1}$ expression, but the introduction of wild or mutant type of p53 expression vector did not induce $p21^{WAF1/CIP1}$ expression. B: HDAC1 depletion did not induce $p21^{WAF1/CIP1}$ expression. C: Western blot analysis of cell cycle components on HDAC1 depletion in A549 cells. The knockdown of HDAC1 did not affect on the expressions of cyclin D1, cyclin E2, and CDK2 in A549 cells. The α-tubulin was used as the protein loading control. All experiments were repeated three times with same results. A typical result of three performed experiments is shown. D: The growth rates of A549 cells exhibited no significant difference between the cells transfected with none (Control), lipofectamine only (Lipo), 100 nmol/L scrambled siRNA (Scr siRNA), 100 nmol/L HDAC1 siRNA, respectively. Error bars indicate mean ± SD of three experiments.

A549 cells. Next, to validate that $p21^{WAF1/CIP1}$ induction is specific to HDAC2, both HDAC2 and HDAC1 were silenced. As shown in Figure 5B, each knockdown of HDAC2 or HDAC1 caused an increase in acetylated histone H3 (Ac-histone H3) demonstrating a major HDAC activity in A549 cells. However, as we expected, it appeared that only HDAC2 knockdown caused $p21^{WAF1/CIP1}$ expression in A549 cells. In addition, HDAC1 knockdown did not affect expression of cyclins and CDKs that were selectively regulated by HDAC2 in A549 cells (Fig. 5C). Furthermore, we also observed that HDAC1 inhibition did not affect the growth rate of A549 cells (Fig. 5D). These results indicated that the oncogenic potential of HDAC2 was exerted by selective regulation of apoptosis and cell cycle proteins by independent of the HDAC1 activity in A549 lung cancer cells.

SUSTAINED SUPPRESSION OF HDAC2 ATTENUATES TUMORIGENIC POTENTIAL OF A549 LUNG CANCER CELLS IN VITRO AND IN VIVO

Our results showed that transient knockdown of HDAC2 caused cellular apoptosis and growth arrest in A549 lung cancer cells. Thus, to investigate whether stable suppression of HDAC2 leads to the suppression of lung tumorigenesis, we established the HDAC2 knockdown cell lines (HD2 KD1 and HD2 KD2) which carrying minimal expression of HDAC2, and confirmed sustained-suppression of HDAC2 activity by detecting $p21^{WAF1/CIP1}$ induction and CDK2/cyclin D1 suppression in established cell lines (Fig. 6A). As transient knockdown of HDAC2 reduced the tumor cell growth rate and de novo DNA synthesis, we firstly assessed the growth rate of these established cell lines. As shown in Figure 6B, HD2 KD1 and HD2 KD2 cells exhibited a reduced growth rate as compared to the mock or control cells. To clarify that this anti-growth effect of established-cell lines (HD2 KD1 and HD KD2) is caused by HDAC2 inactivation in A549 cells, ectopic expression of HDAC2 in established-cell lines was performed. As shown in Figure 6C, introduction of HDAC2 expression plasmid (Flag-HDAC2 vector) successfully caused endogenous expression of HDAC2, and that suppressed $p21^{WAF1/CIP1}$ expression and induced cyclin D1 and CDK2 expressions. Based on this result, we next explored the in vitro tumorigenic assays such as anchorage-independent colony formation and cell motility.

Cancer cells need to acquire the anchorage-independent growth ability for malignant transformation. The results of our study have indicated that overexpression of HDAC2 gave this potential to the cells as suppression of HDAC2 expression displayed a reduced transforming potential in anchorage-independent colony formation assay (Fig. 6D). Acquiring active locomotion and invasion property of neoplastic cells are the other hallmarks of cancer. However, stable knockdown of HDAC2 in A549 cells did not affect on the cell motility (Fig. 6E). Finally, to demonstrate that aberrant regulation of HDAC2 enhances tumorigenic property in vivo, we subcutaneously

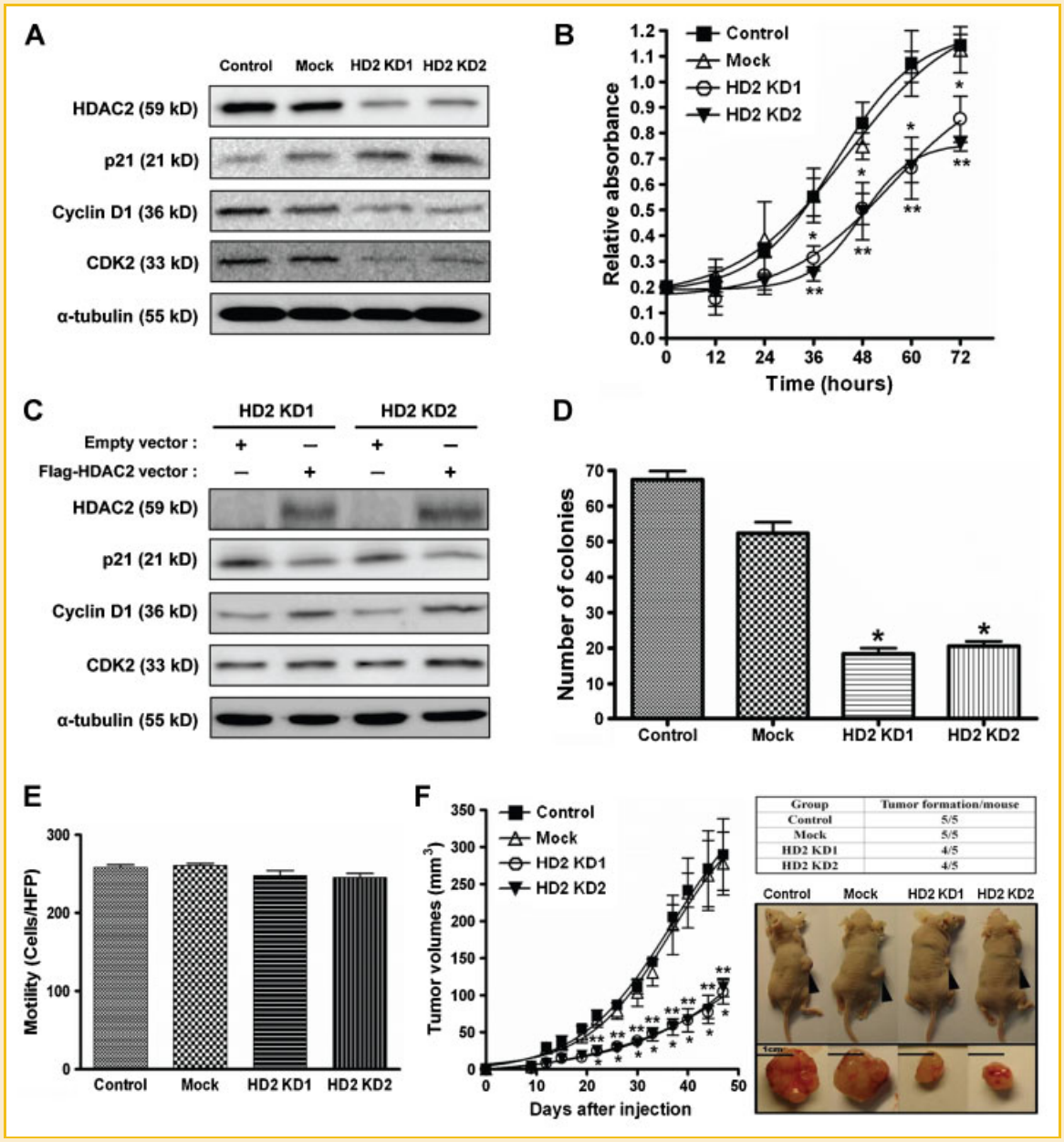

Fig. 6. Sustained suppression of HDAC2 abrogates the tumorigenic potential of A549 human lung cancer cells in vitro and in vivo. A: Establishment of cell lines that sustained limited-HDAC2 expression of A549 cells. Stable cell clones were established by geneticin (G418) using the pSilencer neo expression vector as described in Materials and Methods section. Limited-expression and activity of HDAC2 confirmed by detecting differential expressions of HDAC2, $p21^{WAF1/CIP1}$, cyclin D1, and CDK2 in knockdown cell lines. A typical result of three performed experiments is shown. B: Tumor cell growth rates of A549 cells stably expressing a scrambled shRNA (Mock) and HDAC2 shRNA (HD2 KD1 and HD2 KD2). The relative growth rate was determined by MTT assay at the each indicated time point. The data are presented as mean $\pm$ SD for the three experiments (unpaired Student's *t* test, $^{*,**}P < 0.05$ vs. Mock). C: HDAC2 shRNA (HD2 KD1 and HD2 KD2) cell clones were transfected with empty vector (Mock), or 1 ug of pME18S-Flag-HDAC2 expression vector (Flag-HDAC2 vector). Expression levels of HDAC2, $p21^{WAF1/CIP1}$, cyclin D1, and CDK2 were determined by western blot analysis. The α-tubulin was used as a loading control. D: Analysis of the in vitro soft agar colony assay. Scrambled shRNA (Mock) and HDAC2 shRNA (HD2 KD1 and HD2 KD2) cell clones were cultured in soft agar medium. The data are presented as mean $\pm$ SD of the three experiments (unpaired Student's *t* test, $^{*}P < 0.05$ vs. Mock). E: Cell migration assay was performed by using Boyden chamber system. Each cell lines that migrated through the membranes were fixed, stained, photographed, and counted under light microscopy. The data are presented as the average number of cells migrated in three independent experiments. Error bars indicate mean $\pm$ SD of three experiments. F: In vivo xenograft tumor growth assay. Left panel, the curves represent the mean tumor volumes (calculated from four tumor-bearing mice at each group) of A549 cells stably expressing a scrambled shRNA (Mock) and HDAC2 shRNA (HD2 KD1 and HD2 KD2). Values shown are mean $\pm$ SD, n = 5 for Mock; n = 4 for HD2 KD1 and HD2 KD2 ($^{*,**}P < 0.05$ vs. Mock). Right panel, tumor incidence was noted (table) and the tumors were measured with calipers in three dimensions on the indicated days. Appearances of the representative subcutaneous flank tumor and the sacrificed tumors from the each cell type described were taken at day 47 after inoculation.

injected these established-cell lines into athymic nude mice (Fig. 6F). At 9 days post-inoculation, tumor mass was detectable in the mock or control group. In contrast, in the mice that were injected with HD2 KD1 or HD2 KD2 cells, tumor mass was detectable at 14 days post-inoculation. The overall tumor growth rates significantly resulted in regression of HDAC2 knockdown cell line groups (HD2 KD1 and HD2 KD2). For tumor incidence, the control and mock groups bore five tumors in all the five injected animals, but the HDAC2 knockdown cell lines exhibited four tumors in the five injected animals.

DISCUSSION

Accumulating evidence has suggested that HDACs regulate the expression and activity of numerous proteins involved in both cancer initiation and cancer progression [Glozak and Seto, 2007; Marks et al., 2001a]. Hence, a multitude of HDAC inhibitors have been developed and are currently being tested as anticancer agents in a variety of solid and hematological malignances. However, HDAC inhibitors used to demonstrate effects on cells are for the most part non-specific for the different HDAC isoforms. Thus, only recently research began to focus on the histone acetylation status in human cancers in general and the specific expression of HDAC isoforms in solid as well as hematological malignances, and several studies have shown that certain HDAC family members are aberrantly expressed in several tumors and have non-redundant function in controlling hallmarks of cancer cells [Weichert, 2009; Witt et al., 2009]. Increasing evidence suggested aberrant expression of HDAC2 in neoplastic diseases, and demonstrated that HDAC2 depletion causes growth arrest and apoptosis of certain human cancer cells [Zhu et al., 2004; Huang et al., 2005; Fritsche et al., 2009]. In this study, we have suggested that HDAC2 inactivation augmented cellular apoptosis and arrested the G1/S cell cycle transition in human A549 lung cancer cells, and consequently regressed the tumor cell growth in the xenograft animal model.

In a comprehensive RNA-based study on lung cancer, Osada et al. [2004] found differential expression of HDAC isoforms in NSCLC with the highest expression levels for HDAC1, followed by HDAC3 and HDAC2. It has also been suggested that expression of HDAC2 was associated with large cell type of NSCLC [Borczuk et al., 2003; Shah et al., 2004]. However, no attempt has been made to explain the underlying mechanisms responsible for the mitogenic potential of HDAC2 in lung cancer. We therefore assessed the HDAC2 expression in lung cancer tissues and compared it to the normal tissue using immunohistochemical staining of human lung cancer TMA. Although there were no differences in HDAC2 expression among the histological subtypes of NSCLC, HDAC2 appeared to be deregulated and overexpressed in lung cancer tissues (Fig. 1). We then explored the oncogenic roles of HDAC2 in lung cancer. HDAC2 inactivation by siRNA directed against HDAC2 in A549 lung cancer cells exhibited suppression of tumor cell growth, de novo DNA synthesis and induction of cellular apoptosis (Fig. 2). For the underlying mechanism by which HDAC2 suppresses cellular apoptosis, our results demonstrated that HDAC2 inactivation elicited the induction of p53 and Bax expressions, and concomitantly reduction of Bcl2 expression (Fig. 2D). This result could be partially explained by that overexpression of HDAC2 suppresses p53 expression, which is transcriptional activator of Bax, a pro-apoptotic factor. At the same time, overexpression of HDAC2 also induces Bcl2 expression, a pro-survival factor, so that the transformed cells overcome the apoptotic signal.

Accumulating evidences have suggested that HDAC-mediated repression of genes can cause uncontrolled cell growth as HDACs repress the transcription of cyclin-dependent kinase inhibitors (CDKIs), allowing continued proliferation [Glozak and Seto, 2007]. Our results indicated that HDAC2 knockdown induced the $p21^{WAF1/CIP1}$ expression thereby implying the inhibition of G1/S transition of cell cycle (Figs. 3A and 4B,D). In addition, HDAC2 knockdown suppressed the expression of cyclin E/CDK2 complex. Although it is not clear whether $p21^{WAF1/CIP1}$ directly suppresses the cyclin E/CDK2 complex or HDAC2 directly suppresses it, it is obvious that this synergistic negative regulation of G1/S transition suggests a potent role of HDAC2 in cell cycle regulation. Further, we also confirmed these tumor-suppressor effects of HDAC2 inactivation in other lung cancer cell lines, such as NIC-H358 and NCI-H460 (Fig. 4). This fact strongly supports the role of HDAC2 as a multi-potent regulator of cell growth. Orderly progression through the cell cycle checkpoints involves coordinated activation of the CDKs that in the presence of an associated CDK-activating kinase, phosphorylate target substrates including members of the "pocket protein" family. One of these, the product of the retinoblastoma susceptibility gene (the pRb protein), is phosphorylated sequentially by both the CDK4/cyclin D1 complexes and CDK2/cyclin E kinases. Our results also demonstrated that the resulting suppression of CDK/cyclin complex augmented the hypophoshorylation status of pRb, and suppressed transcriptional activation of E2F/DP1 target genes (Fig. 3C). HDACs function by interacting with the tumor suppressor genes such as p53, Rb, and BRCA1 [Brehm et al., 1998; Yarden and Brody, 1999; Luo et al., 2000]. For example, HDAC1 is necessary for the repression of E2F target genes by Rb [Brehm et al., 1998]. Alternatively, the deacetylation of non-histone proteins such as p53 may also play a role in controlling the cell cycle dynamics. Unlike this suppressor role of HDACs on pRb and its interaction with E2F/DP transcription, our data suggest that HDAC2 act as a potent modulator regulating the expression level of CDK inhibitor, cyclins, and CDKs of the cell cycle circuit, especially in the G1/S transition.

As we observed that the endogenous expression levels of HDAC1 and HDAC2 were relatively high among the HDACs analyzed in lung cancer cells (Fig. 2A), we could not exclude the possible role of HDAC1 in cancer progression in A549 cells. HDAC1 and HDAC2 are shown to be highly homologous and are found together in large protein complexes [Taunton et al., 1996]. However, the regulatory functions of HDAC2 in cell cycle components were not recapitulated by HDAC1 (Fig. 5C). In addition, we found that HDAC2 knockdown induced p53 and $p21^{WAF1/CIP1}$ expression, but HDAC1 did not affect these tumor suppressors. Furthermore, we noted that $p21^{WAF1/CIP1}$ was directly regulated by HDAC2 in a p53-independent manner (Fig. 5A,B).

Although there are some reports that HDAC2 expression is dysregulated in cancer cells, only limited number of articles has shown in vivo functional analysis of HDAC2 in cancer. In this study,

we successfully established stable cell lines with very limited HDAC2 expression level. Experimental mouse xenograft model using these cell lines demonstrated a remarkable suppression of tumor mass growth in vivo. In addition, tumor incidence was lower in the HDAC2 knockdown cell lines which can possibly be explained by the fact that suppression of HDAC2 reduced the anchorage-independent growth ability in vitro (Fig. 6).

In conclusion, we have shown the aberrant expression of HDAC2 in different histologic types of lung cancer tissues. We have also demonstrated that targeted disruption of HDAC2 revealed strong anti-proliferative and pro-apoptotic effects on human lung cancer in vitro and in vivo. Aberrant actions of HDAC2 disturbed homeostasis via dysregulation of gene expression and signaling of apoptosis and cell cycle in lung cells. Detailed analyses of the molecular mechanisms governing gene regulation by HDAC2 will illustrate how this protein influences proliferation, apoptosis, and differentiation of cells. Here, we propose that the aberrant regulation of HDAC2 and its epigenetic regulation of gene transcription in apoptosis and cell cycle components play an important role in the development of lung cancer. This may contribute to tumor cells having mitogenic potential in the development of lung cancer thereby providing novel targets for therapeutic intervention.

ACKNOWLEDGMENTS

This research was supported by Basic Science Research Program through the National Research Foundation of Korea (NRF) funded by the Ministry of Education, Science and Technology (2009-0072504) and by Public Welfare & Safety program through the National Research Foundation of Korea (NRF) funded by the Ministry of Education, Science and Technology (2010-0020764).

REFERENCES

Borczuk AC, Gorenstein L, Walter KL, Assaad AA, Wang L, Powell CA. 2003. Non-small-cell lung cancer molecular signatures recapitulate lung developmental pathways. Am J Pathol 163:1949–1960.

Brehm A, Miska EA, McCance DJ, Reid JL, Bannister AJ, Kouzarides T. 1998. Retinoblastoma protein recruits histone deacetylase to repress transcription. Nature 391:597–601.

Fernandes I, Bastien Y, Wai T, Nygard K, Lin R, Cormier O, Lee HS, Eng F, Bertos NR, Pelletier N, Mader S, Han VK, Yang XJ, White JH. 2003. Ligand-dependent nuclear receptor corepressor LCoR functions by histone deacetylase-dependent and -independent mechanisms. Mol Cell 11:139–150.

Fritsche P, Seidler B, Schuler S, Schnieke A, Gottlicher M, Schmid RM, Saur D, Schneider G. 2009. HDAC2 mediates therapeutic resistance of pancreatic cancer cells via the BH3-only protein NOXA. Gut 58:1399–1409.

Glozak MA, Seto E. 2007. Histone deacetylases and cancer. Oncogene 26:5420–5432.

Gregoretti IV, Lee YM, Goodson HV. 2004. Molecular evolution of the histone deacetylase family: Functional implications of phylogenetic analysis. J Mol Biol 338:17–31.

Huang BH, Laban M, Leung CH, Lee L, Lee CK, Salto-Tellez M, Raju GC, Hooi SC. 2005. Inhibition of histone deacetylase 2 increases apoptosis and p21Cip1/WAF1 expression, independent of histone deacetylase 1. Cell Death Differ 12:395–404.

Johnstone RW. 2002. Histone-deacetylase inhibitors: Novel drugs for the treatment of cancer. Nat Rev Drug Discov 1:287–299.

Kononen J, Bubendorf L, Kallioniemi A, Barlund M, Schraml P, Leighton S, Torhorst J, Mihatsch MJ, Sauter G, Kallioniemi OP. 1998. Tissue microarrays for high-throughput molecular profiling of tumor specimens. Nat Med 4: 844–847.

Kortenhorst MS, Carducci MA, Shabbeer S. 2006. Acetylation and histone deacetylase inhibitors in cancer. Cell Oncol 28:191–222.

Luo J, Su F, Chen D, Shiloh A, Gu W. 2000. Deacetylation of p53 modulates its effect on cell growth and apoptosis. Nature 408:377–381.

Marks P, Rifkind RA, Richon VM, Breslow R, Miller T, Kelly WK. 2001a. Histone deacetylases and cancer: Causes and therapies. Nat Rev Cancer 1:194–202.

Marks PA, Richon VM, Breslow R, Rifkind RA. 2001b. Histone deacetylase inhibitors as new cancer drugs. Curr Opin Oncol 13:477–483.

Minucci S, Pelicci PG. 2006. Histone deacetylase inhibitors and the promise of epigenetic (and more) treatments for cancer. Nat Rev Cancer 6:38–51.

Noh JH, Eun JW, Ryu SY, Jeong KW, Kim JK, Lee SH, Park WS, Yoo NJ, Lee JY, Nam SW. 2006. Increased Expression of Histone Deacetylase2 is Found in Human Hepatocellular Carconoma. Mol Cell Toxicol 2:166–169.

Osada H, Tatematsu Y, Saito H, Yatabe Y, Mitsudomi T, Takahashi T. 2004. Reduced expression of class II histone deacetylase genes is associated with poor prognosis in lung cancer patients. Int J Cancer 112:26–32.

Shah L, Walter KL, Borczuk AC, Kawut SM, Sonett JR, Gorenstein LA, Ginsburg ME, Steinglass KM, Powell CA. 2004. Expression of syndecan-1 and expression of epidermal growth factor receptor are associated with survival in patients with nonsmall cell lung carcinoma. Cancer 101:1632–1638.

Song J, Clair T, Noh JH, Eun JW, Ryu SY, Lee SN, Ahn YM, Kim SY, Lee SH, Park WS, Yoo NJ, Lee JY, Nam SW. 2005a. Autotaxin (lysoPLD/NPP2) protects fibroblasts from apoptosis through its enzymatic product, lysophosphatidic acid, utilizing albumin-bound substrate. Biochem Biophys Res Commun 337:967–975.

Song J, Noh JH, Lee JH, Eun JW, Ahn YM, Kim SY, Lee SH, Park WS, Yoo NJ, Lee JY, Nam SW. 2005b. Increased expression of histone deacetylase 2 is found in human gastric cancer. APMIS 113:264–268.

Taunton J, Hassig CA, Schreiber SL. 1996. A mammalian histone deacetylase related to the yeast transcriptional regulator Rpd3p. Science 272:408–411.

Weichert W. 2009. HDAC expression and clinical prognosis in human malignancies. Cancer Lett 280:168–176.

Witt O, Deubzer HE, Milde T, Oehme I. 2009. HDAC family: What are the cancer relevant targets? Cancer Lett 277:8–21.

Yang XJ, Seto E. 2007. HATs and HDACs: From structure, function and regulation to novel strategies for therapy and prevention. Oncogene 26: 5310–5318.

Yarden RI, Brody LC. 1999. BRCA1 interacts with components of the histone deacetylase complex. Proc Natl Acad Sci USA 96:4983–4988.

Zhang Y, Ng HH, Erdjument-Bromage H, Tempst P, Bird A, Reinberg D. 1999. Analysis of the NuRD subunits reveals a histone deacetylase core complex and a connection with DNA methylation. Genes Dev 13:1924–1935.

Zhu P, Martin E, Mengwasser J, Schlag P, Janssen KP, Gottlicher M. 2004. Induction of HDAC2 expression upon loss of APC in colorectal tumorigenesis. Cancer Cell 5:455–463.